ELSEVIER

Journal of Alloys and Compounds 293–295 (1999) 107–112

Journal of ALLOYS AND COMPOUNDS

Structure study on rapidly solidified hydrogen storage alloy $Zr(NiM)_{2.1}$

G.L. Lü[a,*], K.Y. Shu[b], L.S. Chen[a], X.Y. Song[b], X.G. Yang[b], Y.Q. Lei[b], Q.D. Wang[b]

[a]*Central Laboratory, Zhejiang University, Hangzhou 310028, China*
[b]*Department of Mater. Sci. and Eng., Zhejiang University, Hangzhou 310027, China*

Abstract

Molten alloy $Zr(NiM)_{2.1}$ (M=Mn, Cr, V) is rapidly solidified by melt spinning method with cooling rates of alloy ribbons between 4.35×10^5 Ks^{-1} and 5.33×10^6 Ks^{-1}. The structure is analyzed by means of XRD and TEM. The data from XRD are further analyzed by the Rietveld method. The results show that all the rapidly solidified alloys with different cooling rates are composed only of micro-crystalline C14 Laves and C15 Laves phases, different from the appearance of the non-Laves phase constituents Zr_7M_{10} and Zr_9Ni_{11} together with the C14 and C15 Laves phase in the slowly cooled master alloy. The C14 Laves phase in rapidly solidified alloys assumes a laminar structure, in which the dimensions of C14 Laves micro-crystallites are almost constant, 1 nm along the *c* direction and 3–4 nm along the *a* and *b* directions. The abundance of C14 Laves phase increases in rapidly solidified alloys as the cooling rate increases, and on the contrary, the abundance of C15 Laves phase decreases. When the cooling rate increases from 4.35×10^5 Ks^{-1} to 5.33×10^6 Ks^{-1}, the abundance of C15 Laves phase decreases from 88.29 wt.% to 43.63 wt.%, and the crystallite size of C15 phase decreases from 54.1 nm to 17.8 nm.

Keywords: Rapidly solidified hydrogen storage alloys; Laves phase; Rietveld analysis

1. Introduction

It is well known that annealed and rapidly solidified alloys would be more homogeneous in composition, with improved microstructures and improved physical and chemical properties. Generally after annealing or rapid solidification, the microstructures of many single phased metal hydrogen storage alloys are changed, and their electrochemical properties improved, yet they still maintain the single phase structure, for example still of $CaCu_5$ type [1]. Cast Zr-based pseudo-binary hydrogen storage alloys are multiphase alloys that contain AB_2 type Laves phases and AB_{2-x} type non-Laves phases. Electrochemical properties of such alloys are closely related to the phase composition which in turn are related to the components and combinations in B-side [2]. Nickel is the indispensable B component of all Zr-based AB_2 type electrode alloys, and is also the element for forming non-Laves phases [3]. Phase composition is changed by annealing treatment, which generally worsens the electrochemical properties [4]. There thus exists a complex relationship between electrochemical properties and phase composition.

In this paper, we studied the relationship between phase composition and electrochemical properties of a Zr-based AB_2 type pseudo-binary alloy by means of a rapid solidification method — melt-spinning with a single roller at different cooling rates.

2. Experimental

2.1. Sample preparation

The master alloy consists of Zr, Ni, Cr, Mn and V elements with purity all above 99.95%. The formula of the alloy is $Zr(MNi)_{2.1}$ (M=Mn, Cr, V). Alloys were melted repeatedly in vacuum arc furnace for four times on a copper crucible cooled by water. The cooling rate was below 200 Ks^{-1}. The master alloy was re-melted in a quartz crucible and rapidly solidified on a rotating copper roller, the melt spinning method. The cooling rate of alloy ribbons was between 4.35×10^5 Ks^{-1} and 5.33×10^6 Ks^{-1}. The ribbons were ground into powder mechanically and used as experimental samples.

*Corresponding author.

0925-8388/99/$ – see front matter
PII: S0925-8388(99)00308-4

2.2. XRD and TEM analysis

XRD data for Rietveld analysis were obtained at 25°C on a horizontal Rigaku D/max-IIIB powder diffractometer, using CuK_α radiation and a power of 40 kV×30 mA, with a diffracting beam monochrometer over the range 20—120° 2θ with a step interval of 0.02° 2θ and a count time of 5 s per step.

BaF_2, which was annealed at 500°C for 2 hours in air atmosphere, was used as a non-intrinsic broadening sample to measure the instrument function and to extract the alloy's micro-structure data [5].

The morphology and electron diffracted patterns for rapidly solidified alloy with a cooling rate of 3.92×10^6 Ks^{-1} were observed and analyzed using a Philips CM12 TEM.

2.3. Extraction of micro-structural parameters

The micro-structural parameters of samples were determined by means of Rietveld analysis combined with Fourier analysis for broadening peaks. The phenomenological relationship, describing the trend of profile width and shape as a function of diffraction angle as popular Rietveld refinement routines, was replaced by fitting parameters of crystallite size, shape and micro-strain. The fitting parameters were transformed to the parameters of the pseudo-Voigt (pV) function by inverting the Warren–Averbach procedure for a single peak. Then the experimental data were fitted. The anisotropy of size and strain that results in the profile broadening in a different manner with different Miller indices was also considered by introducing two size–strain parameter tensors into the model. Parameter tensors here are similar to the method used in the temperature factor. Some constraint was applied according to the symmetry properties of the crystal [6].

Rietveld refinements of all samples were performed on a 586 PC computer with LS1 software [7].

3. Results and discussion

3.1. Phase composition

Fig. 1 shows the XRD patterns of alloys. The cooling rate of samples decreases from the bottom to the top of the figure. There are obvious differences in XRD patterns between slowly and rapidly solidified alloys. The patterns of rapidly solidified alloys contain two kinds of profile. One is a dispersion micro-crystallite profile, another is a sharp peak belong to C15 Laves phase. But the diffraction intensity of micro-crystallite and the amount of alloy transformed into C15 Laves phase decreased as the cooling rate decreased. There are a lot of sharp peaks in slowly solidified alloy XRD patterns. Fig. 2 shows the Rietveld analysis pattern of slowly solidified alloy samples, which is composed of C15 and C14 Laves phase, Zr_7M_{10} and Zr_9M_{11} non-Laves phases and monoclinic ZrO_2, a typical composition of Zr-based pseudo-binary hydrogen storage alloy.

The peak positions and relative intensity for micro-crystallite indicate that C14 Laves phase is the predominant phase. Fig. 3 shows electron diffraction patterns of rapidly solidified alloy with a cooling rate of 3.92×10^6 Ks^{-1} in two selected areas. The distribution of diffracted dots indicates hexagonal and cubic symmetry respectively. Calculated results show that $a=0.50$ nm, $c=0.81$ nm for patterns of hexagonal symmetry, and $a=0.71$ nm for cubic symmetry.

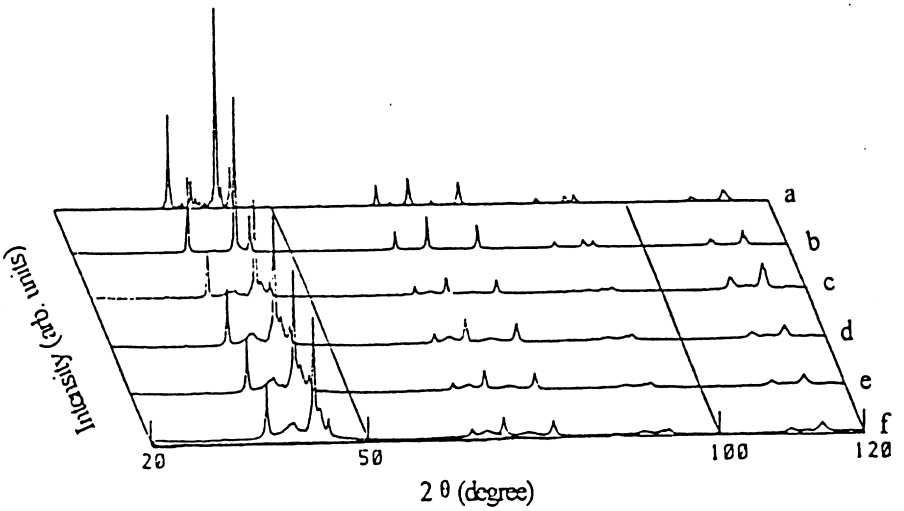

Fig. 1. XRD patterns of master alloy and rapidly solidified alloys. a) master alloy, cooling rate below 200 Ks^{-1}; b) cooling rate 4.35×10^5 Ks^{-1}; c) cooling rate 1.38×10^6 Ks^{-1}; d) cooling rate 2×10^6 Ks^{-1}; e) cooling rate 3.92×10^6 Ks^{-1}; f) cooling rate 5.33×10^6 Ks^{-1}.

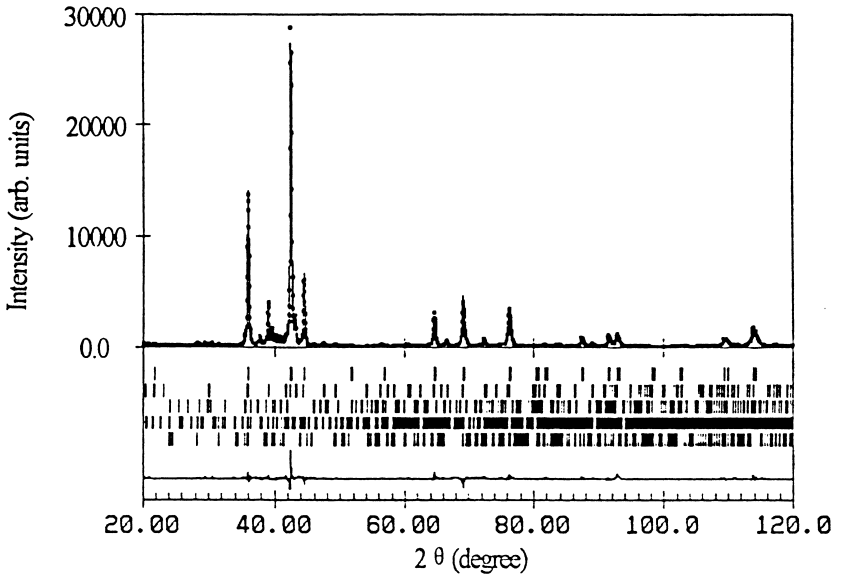

Fig. 2. The observed, calculated, and difference of CuK_{α} X-ray powder diffraction patterns for slowly solidified alloy composed of five phases. The tick marks below the patterns represent the positions of all possible Bragg reflections. They are C15, C14, Zr_9M_{11}, Zr_7M_{10}, ZrO_2 from the top to the bottom respectively.

3.2. Phase abundance and characteristics of microstructure

Fig. 4 shows XRD Rietveld analysis patterns of rapidly solidified alloys with the cooling rate of 4.35×10^5 $Ks^{-1}$and 5.33×10^6 Ks^{-1}, respectively. The calculated pattern matches the experimental pattern very well in the entire range, indicating the selected structure model for the refinement is correct. In this refinement, structure models of C14 and C15 Laves phase were adopted on the basis of their different symmetries. An anisotropic microstructure model was adopted for C14 Laves phase and an isotropic microstructure model for C15. Table 1 lists the numerical results of fitting criteria for all samples. The value of fitting index is in the scope of general Rietveld analysis [8]. These results indicate the model and results are reliable.

The results of phase abundance, microstructure parameters and cell parameters for master alloy and rapidly

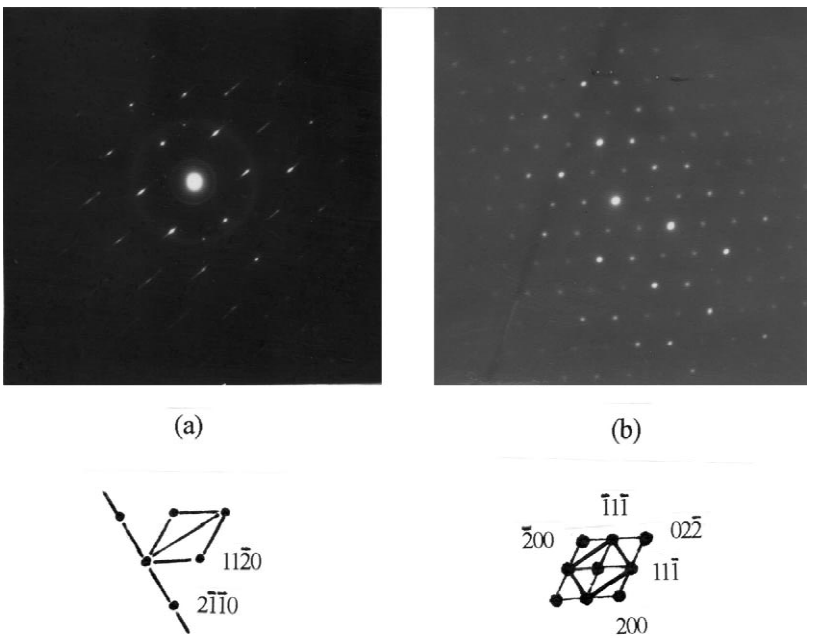

Fig. 3. The selected area electron diffracted patterns for rapidly solidified alloy. a) Hexagonal symmetry, oriented along the $[0\bar{1}13]$ direction. b) Cubic symmetry, oriented along the [011] direction.

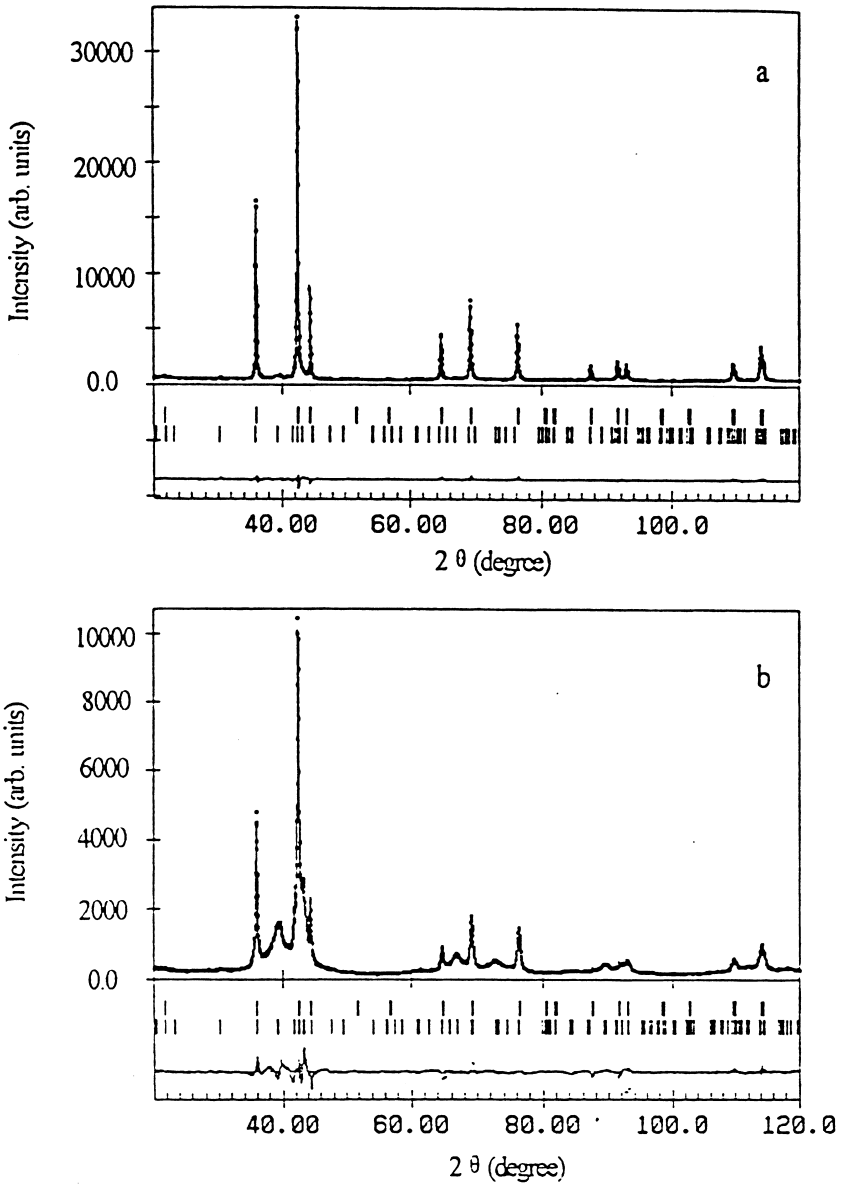

Fig. 4. Observed (dots), calculated (line), and difference (line) results of CuK_{α} X-ray powder diffraction patterns for C14, C15 Laves. a) cooling rate below 200 Ks^{-1}; b) cooling rate 5.33×10^{6} Ks^{-1}.

Table 1
The fitting index of Rietveld analysis for master alloy and rapidly solidified alloys[a]

Cooling rate	R_{wp}	R_p	S	R_B	
Ks^{-1}				C14	C15
<200	10.72	7.94	2.41	6.69	3.40
4.35×10^{5}	5.47	4.21	1.60	6.23	3.17
1.38×10^{6}	7.49	5.76	1.81	6.69	3.79
2.0×10^{6}	13.47	10.15	2.68	4.82	7.79
3.92×10^{6}	12.59	9.76	2.52	4.06	8.15
5.33×10^{6}	11.33	8.67	2.37	3.19	7.54

[a] Note: R_{wp}=weighted pattern factor; R_p=pattern factor; R_B=Bragg factor; S=Goodness of fit.

solidified alloys of different cooling rates are listed in Tables 2 and 3. It is clearly shown that a rapid solidification process leads to the formation of a metastable micro-crystallite C14 Laves phase. The abundance of micro-crystallite C14 phase decreases and C14 transforms into C15 Laves phase as the cooling rate decreases. But the microstructure characteristics are almost invariable. Fig. 5 shows the TEM image of alloy at a cooling rate of 3.92×10^{6} Ks^{-1}. It is clearly shown that TEM image has two different morphologies. One is of lamellar structure, and another is of homogeneous appearance corresponding to micro-crystallite C14 Laves and C15 Laves phase, respectively. A particularly interesting lamellar characteristic of micro-crystallite is consistent with the results of

Table 2
The phase abundance and cell parameters for master alloy and rapidly solidified alloys

Cooling rate	Abundance (wt.%)		Cell parameters (nm)		
Ks^{-1}	C14	C15	C15	C14	
			a	*a*	*c*
<200	9.72(1.3)	72.77(1.71)	0.70580(1)	0.50057(3)	0.81750(6)
4.35×10^5	11.73(2.1)	88.29(1.8)	0.70591(1)	0.50044(192)	0.80957(71)
1.38×10^6	49.94(2.52)	51.06(2.42)	0.70446(2)	0.50214(74)	0.81004(34)
2.0×10^6	48.10(1.5)	51.90(1.99)	0.70502(2)	0.49941(43)	0.81251(22)
3.92×10^6	54.64(1.90)	45.33(1.79)	0.70513(2)	0.49947(44)	0.81196(22)
5.33×10^6	56.37(1.98)	43.63(1.76)	0.70535(2)	0.50029(45)	0.81333(22)

Table 3
The crystallite size and micro-strain for rapidly solidified alloys[a]

Cooling rate	C15		C14			
Ks^{-1}	M_{nn} (nm)	$\langle e^2\rangle_{nn}^{1/2}$	M_{nn} (nm)	$\langle e^2\rangle_{nn}^{1/2}$	M_{nn} (nm)	$\langle e^2\rangle_{nn}^{1/2}$
<200	62.8(1)	0.0013(4)	17.2(5)	0.00001	6.9(3)	0.00001
4.35×10^5	54.1(4)	0.0003(1)	3.3(5)	0.00001	1.02(8)	0.0035
1.38×10^6	31.6(10)	0.0012(2)	3.0(1)	0.00001	0.99(2)	0.0025
2.0×10^6	26.9(1)	0.0017(3)	4.2(4)	0.00001	1.08(2)	0.0028
3.92×10^6	4.2(5)	0.0013(3)	3.7(2)	0.00001	1.18(2)	0.0030
5.33×10^6	17.8(5)	0.0014(2)	3.6(2)	0.00001	1.02(2)	0.0024

[a] Note: subscript $nn=11=22=33$ for C15, along *a*, *b*, *c* axis directions respectively. $nn=11=22$ for C14, along *a*, *b* axis directions, 33 along *c* axis direction.

Rietveld analysis presented in Table 3. The crystallite is only 1 nm in the *c*-axis direction and 3~4 nm in the *a*- and *b*-axis directions. All these results indicate that the flake-like crystallites of rapidly solidified ribbons are of lamellar structure.

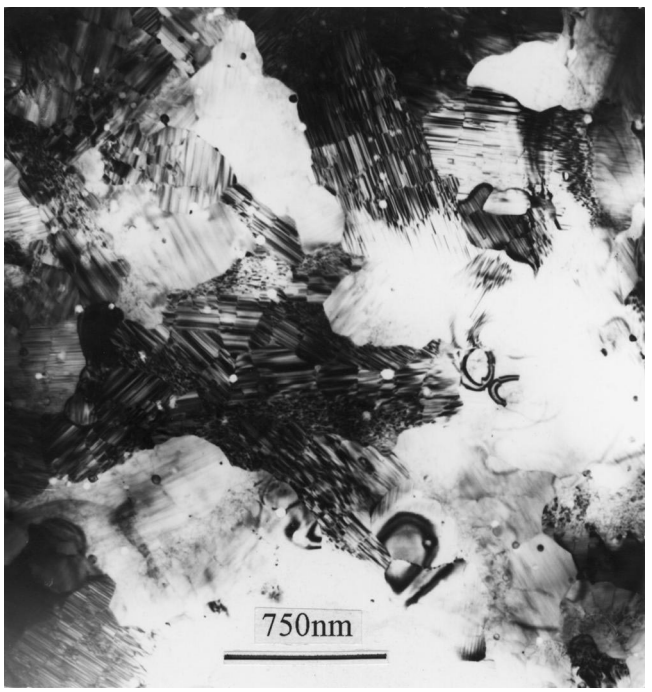

Fig. 5. TEM images of rapidly solidified alloys showing the presence of two different morphological regions, lamellar and homogeneous.

It should be noted that C14 Laves phase of rapidly solidified alloys is different from that of its master alloy either in formation mechanism or structure characteristics. The micro-crystallite C14 Laves phase is a metastable phase. It coexists with C15 Laves phase within a certain cooling rate range. We believe that the alloy is entirely micro-crystalline above a certain cooling rate. On the contrary, it is only C15 Laves phase as the cooling rate is lowered into certain range. But when the cooling rate is lowered still more, component segregation will occur, with the appearance of non-Laves phase and C14 Laves again, as happened in the slowly cooled master alloy.

3.3. Electrochemical properties

The electrochemical properties were tested in standard tri-electrode cells. The results indicate that electrochemical properties are closely related to the phase composition and microstructure of the rapidly solidified alloy. The experimental results also show that the discharge capacity of multiphase as-cast alloy is 300 $mAhg^{-1}$, lower than that of the rapidly solidified alloy cooled at about 4.43×10^5 Ks^{-1} containing mainly C15 Laves phase. But when the cooling rate of rapidly solidified alloy reaches 5.53×10^6 Ks^{-1}, it contains only 43.63 wt.% C15 Laves phase, and its discharge capacity drops to 260 $mAhg^{-1}$.

The cycle life of the rapidly solidified alloy is much longer than that of the as-cast alloy. And the higher the cooling rate of rapidly solidified alloy, the longer the cycle life is due to the increase of micro-crystallite C14 Laves

phase. The above results indicate that there exists a definite relationship between the rapid solidification process and electrochemical properties. Details are reported elsewhere [9].

4. Conclusions

Rapidly solidified (melt-spun) pseudo-binary alloy $Zr(NiM)_{2.1}$ is composed of micro-crystallite C14 Laves phase and C15 Laves phase. The abundance of micro-crystallite C14 Laves phase decreases as the cooling rate of rapidly solidified alloy is lowered, and at the same time, the abundance of C15 Laves phase increases. The micro-crystallite C14 Laves assumes a flake-like shape. The existence and abundance of micro-crystallite C14 Laves have great effects on the alloy's electrochemical properties.

Acknowledgements

This work was supported by National and Zhejiang Provincial Natural Science Foundation of China (No. 59671016, 59601006, 594100) and the National Advanced Material Committee of China (No. 715-004-0060).

References

[1] W. Tang, G. Sun, J. Alloys Comp. 203 (1994) 195.
[2] S.R. Ovshinsy, M.A. Fetcenko, Russ J. Sci. 176 (1993) 260.
[3] X.R. Hu, J.M. Gu, L.S. Chen, G.L. Lu, W.K. Zhang, Y.Q. Lei, Q.D. Wang, Chinese Journal of Material Research, to be submitted.
[4] W.K. Zhang, Dissertation Submitted to Zhejiang University for the Degree of Doctor of Philosophy, 1997, pp. 76—85.
[5] D. Louêr, J.I. Langford, J. Appl. Cryst. 21 (1988) 430.
[6] L. Lutterotti, R. Scardi, J. Appl. Cryst. 23 (1990) 246.
[7] L. Lutterotti, R. Scardi, J. Appl. Cryst. 25 (1992) 459.
[8] E. Prince, The Rietveld Method, in: R.A. Young (Ed.), Oxford University Press, Oxford, 1993.
[9] K.Y. Shu, Y.Q. Lei, X.G. Yong, G.F. Lin, Q.D. Wang, G.L. Lu, L.S. Chen, Effect of Rapidly Solidified Process on the Alloy Structure and Electrochemical Performances of $Zr(NiMnM)_{2.1}$, International Symposium on Metal–Hydrogen Systems, Fundamental and Application, Oct. 4–9, 1998, Hangzhou, China.